JOURNAL OF AIRCRAFT
Vol. 44, No. 1, January–February 2007

Drag and Flutter Characteristics of Loop Membranes

Anna C. Carruthers* and Antonio Filippone†
University of Manchester, Manchester, M60 1QD England, United Kingdom

DOI: 10.2514/1.23679

We present the results of experimental investigations on the aerodynamic characteristics of high-drag devices with flexible membranes joined at their short ends (*loops*). The loops were placed in a low-speed wind tunnel and tested at speeds up to 19 m/s. The range of Reynolds numbers was $Re = 2 \times 10^5$–2×10^6. The loops were tested for a variety of aspect ratios, from 3.3 to 30, three planform areas, and two mounting methods. Results are presented for the drag coefficient and for the flutter characteristics. We prove that with a low aspect ratio the loops form a teardrop shape and their flutter mode is a sinusoidal-like oscillation. Furthermore, the drag coefficient decreases with the increasing wind speed, but it depends strongly on the aspect ratio and the planform area. Empirical correlations for the drag coefficient are polynomial equations.

Nomenclature

A	=	planform area, m^2
C_D	=	drag coefficient based on the planform area (single side area)
c_1, c_2	=	coefficients in Eq. (1)
Re	=	Reynolds number based on loop length
U	=	freestream velocity, m/s
τ	=	loop thickness, mm

Introduction

LOOPS belong to a class of aerodynamic systems that can be called decelerators, because of the relatively high drag they create. They are flaglike devices made of a slender strip with the luff and leech attached to the same point. The high degree of flexibility that they offer results in a canopy shape that depends on the planform geometry and the wind characteristics (speed and turbulence). Most commonly rectangular in shape, the simple geometry makes them cheap and easy to manufacture. Loops are part of a family of flexible membranes of interest in aerodynamics, including wings, paragliders, streamers, and flight stabilizers.

In the past, loops have been applied to the stabilization of rocket-launched grenades. Following deployment, grenades tend to suffer large-amplitude oscillations that dampen out once the loop unwinds. The secondary effect is to decelerate the grenade to a terminal velocity. A range of wind-tunnel, gun-launched, and open-air drop tests have been performed by Auman et al. [1]. It has been found that in the high-velocity testing range (80–150 ft/s) varying testing methods will yield correlating results. These high testing velocities all ensure a relatively straight canopy to the loop, but it is not at all clear from the current information whether results obtained at much lower velocities will concur with these previous experiments. Other devices applied in the past for the stabilization of air-launched weapons include feathered dartlike bombs (*flechette*).

There is a strong relevance of these loop membranes to the modeling of collapsed high-drag aerodynamic systems such as parachutes and paragliders. The collapse of such systems can be disastrous for a human or fragile payload, and little is known about the drag properties of these systems. Loops are a simplistic approximation of these more complex systems but can therefore provide some insight into the behavior of the higher drag systems under canopy collapse. The information currently available on loops is relatively limited and encompasses the high-speed regime only. Initial observations indicate that loops do not exhibit similar behavior at low and high velocities, which makes low-speed testing the primary interest of this study.

The research presented in this paper addresses the aerodynamic characteristics (drag and flutter) of the loops at low speeds. In recent years, the flexible membrane problems have been the subject of increasing modeling and simulation efforts. When the membranes are roughly aligned with a laminar or turbulent flow, the use of the Navier–Stokes equations provides reasonable prediction of the aerodynamic coefficients over a wide range of inflow angles [2]. The problem that will be described in this paper consists of highly flexible membranes that are subject to large-amplitude deformations and flutter. At high speeds, loops suffer low-amplitude high-frequency oscillations. Furthermore, the shape assumed by the loops cannot be reasonably predicted. Therefore, the research is of an experimental nature.

It has been found that at a given velocity the region of significant flutter moves tailward with the increasing length of the loop. This means that longer loops, which would suffer only large-amplitude oscillations over a smaller fraction of their length, will transmit less disturbance towards the luff, and hence the payload. This fact was first demonstrated by Auman and Dahlke [3]. Empirical formulas for streamers and loops have been determined to describe the variation of the drag coefficient with the aspect ratio [4]:

$$C_D = 0.2988\mathrm{AR}^{-0.5599}, \qquad \tau = 0.28 \text{ mm}$$

$$C_D = 0.4790\mathrm{AR}^{-0.6801}, \qquad \tau = 0.43 \text{ mm}$$

The drag characteristics have been measured for nylon loops (material properties not specified) and remain valid over two velocity ranges, $27 \text{ m/s} < U < 46 \text{ m/s}$ and a higher range of $280 \text{ m/s} < U < 600 \text{ m/s}$. The shape of the loop canopy at these relatively high velocities is streamerlike, i.e., they tend to fold and appear as a flag; however, at a low velocity this is not the case, and no data currently exist that attempts to describe the various motions experienced by the loops in this low-speed regime.

The inclusion of material properties has not, to date, been dealt with in consideration of loops. However, research concerning the closely related "streamer" decelerators has touched on this subject [5–7]. Levin et al [6] have shown that, in reference to streamers and flags, the drag characteristics of streamers are directly affected by its material properties. The effects of cloth properties on the drag and flutter characteristics of loops are certainly an area for further research. Therefore, the study conducted here attempts to incorporate

Received 6 March 2006; revision received 4 August 2006; accepted for publication 31 August 2006.

*Ph.D. student, School of Mechanical, Aerospace, Civil Engineering, currently at Flight Group, Department of Zoology, University of Oxford, South Parks Road, Oxford, OX1 3PS England, United Kingdom.

†Lecturer, School of Mechanical, Aerospace, Civil Engineering, George Begg Building, P.O. Box 88; a.filippone@manchester.ac.uk. Senior Member AIAA (corresponding author).

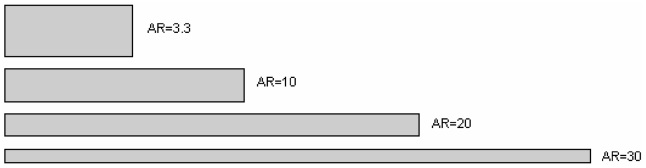

Fig. 1 Loop planforms have all combinations of four aspect ratios and three areas.

the effects of material properties by testing pure cotton of relatively similar material thickness, rather than the nylon cloth previously considered [1,3,4].

Experimental Setup

Tests were conducted in a low-speed wind-tunnel facility at the University of Manchester, which has a working section of 0.92 m^2. The wind-tunnel velocity range is between 6 and 19 m/s and was measured by a pitot–static probe placed near the inlet of the working section. A digital manometer gave the probe output, under varying velocity conditions, enabling accuracies of ± 0.01 mm H_2O at $U =$ 6 m/s to ± 0.18 mm H_2O at 19 m/s to be achieved, giving velocity accuracies of between ± 0.01 and ± 0.08 m/s, respectively. The models were mounted halfway down the wind-tunnel working section, with the pitot–static probe placed at 1/3 of the working section length. The probe position was not adjusted throughout testing, due the length of the larger loops when in position requiring that the probe be upstream of the loops. A separate set of tests were conducted with all models removed from the working section. These tests indicated that the velocity measurement and accuracy, as calculated from dynamic pressure readings, were a fair indication of the velocity properties along the working section length.

Twelve rectangular loops were made of pure cotton (average weight of 177 g/m^2 and bending rigidity of 0.0642 $g \cdot cm/cm$, $\tau = 0.3$ mm). The geometries included all the combinations of four aspect ratios (AR = 3.3, 10, 20, and 30) and three planform areas ($A = 0.025$, 0.050, and 0.075 m^2). These planforms are shown in Fig. 1.

Force measurements were taken using a three-component balance, one component being used to measure the drag. The other two components measured fore and aft lift forces but were not used during this study. The force balance readout was taken as a voltage series through a computer link. This was done because the force balance alone gave instantaneous force measurements only, and the requirement was for an average over a discrete time interval. Data were collected over a 5.12 s interval; 2,048 samples were taken at a frequency of 400 Hz. The final drag coefficients presented are the averages of six test runs taken at each data point. The accompanying error bars indicate the maximum deviations from this average of those six tests. The measured drag is a total of the mounting rod and loop drag; therefore, the presented results have had the mounting rod drag subtracted.

The loops were mounted using a U-shaped mounting rod with a diameter of 12 mm, as shown in Fig. 2b, and were positioned centrally in the tunnel working section. A counterbalance system was employed to relieve the force balance; the force balance becomes insensitive to smaller loads when an initial load (such as a heavy mounting rod) has been applied. The presence of a mounting rod with a 12-mm diameter in front of the loops will of course affect the loop aerodynamics. To compare the drag force data, a second series of tests using a 6-mm horizontal mounting rod was conducted. This was a lightweight rod, and therefore required no counterweight system, that was used to compare data from a selection of loops covering the full area and aspect-ratio range. There was good agreement between the results obtained indicating that the U-shaped mounting rod had a limited effect of the drag and flutter characteristics.

Results and Discussion

Loops undergo two main types of oscillation: flapping and rotational. The flapping mode of oscillation occurs in the x–y plane, with the rotational mode occurring about the x axis, Fig. 3. The rotational mode is not pure rotation, given that the loop ends are fixed, but this motion describes a tendency of the loops towards rotation. Low-aspect-ratio loops do not show obvious signs of the rotational mode, instead appearing to exhibit the flapping mode

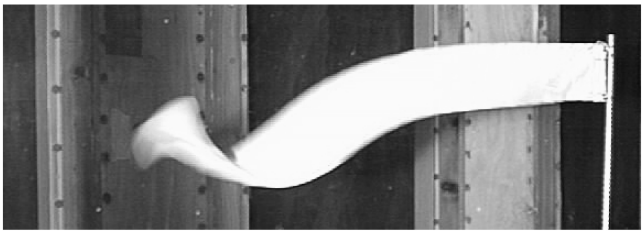

a) Photograph of loop A = 0.075 m^2, AR = 20, U = 6.6 m/s, and Re = 5.5 x 10^5

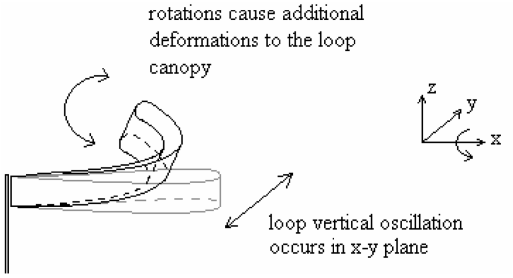

b) Breakdown of loop oscillations into rotational and flapping flutter

Fig. 3 Details of the loop oscillations.

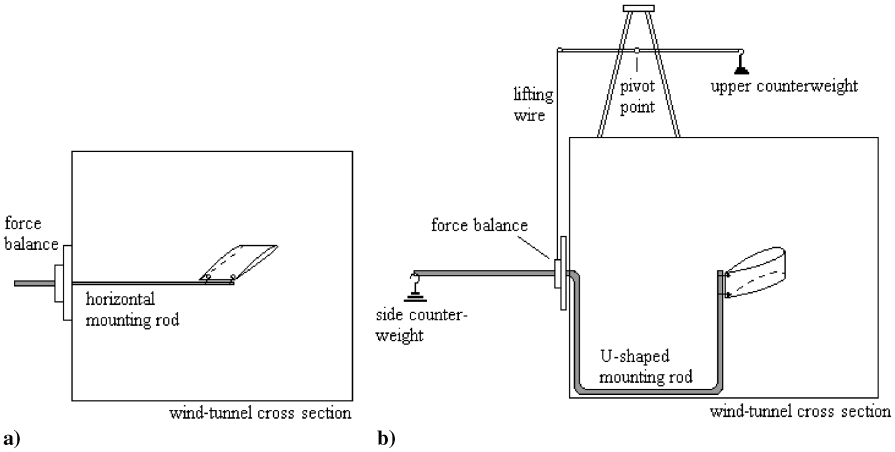

Fig. 2 Horizontal and U-shaped mounting methods.

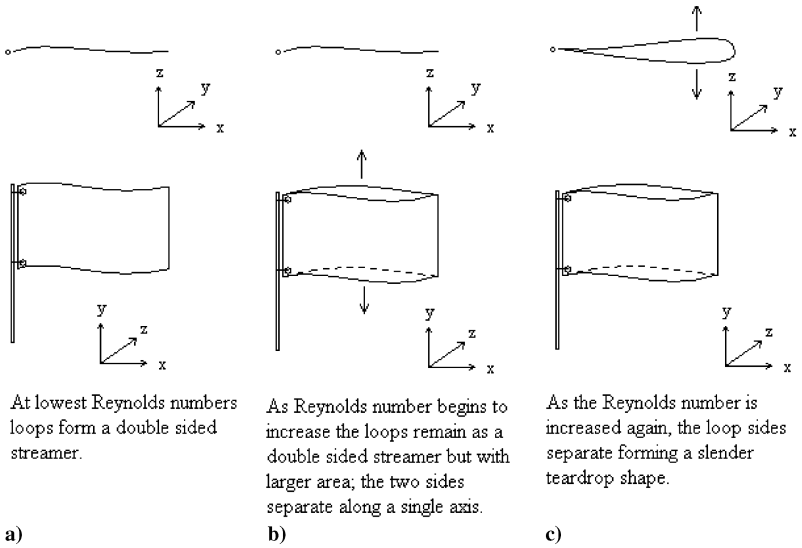

Fig. 4 Shape change of loop with increasing Reynolds number.

alone. Under these conditions the loops tend to fold at the decelerator midline leaving a sharp crease that remains visible when examined afterwards, Fig. 4a. For these devices, the width is the dominant parameter that causes damping of rotations. The rotational tendency of the loop leech will tend to only become visibly apparent for the longer loops.

At these low aspect ratios and areas the loops do not appear to take up a sinusoidal shape but form a section of a sine wave, Fig. 5a. The fluid viscous forces and tension in the loop serve to keep the shape taut; deflections may be of a large amplitude, but the loop moves as a straight flag or as one with only a minor degree of curvature. The flutter mode is therefore a high-amplitude relatively low-frequency oscillation at a low velocity. As the velocity is increased the flutter becomes increasingly violent. The frequency increases but oscillations reduce only slightly in amplitude. A high degree of turbulence and a large wake results in the loop path.

As the aspect ratio is increased, the effect of the rotational mode of oscillation becomes increasingly evident, the end tracing out a figure-eight-like pattern. The decrease in the ratio of fixed edge length (width) to free edge length (length) has the consequence that the rotational mode of oscillation is no longer damped out to the same extent. As the aspect ratio is increased to $AR = 10$, a slight separation of the material on the two sides of the loop is observed, Fig. 4b. The "flaglike" shape remains two-dimensional, but a wider streamer is effectively formed. As the area and aspect ratio are increased, the two sides of the loop separate slightly such that the beginning of a slender teardrop shape is formed, Fig. 4c. The loops now flutter in a sinusoidal-like motion, Fig. 5b. The high-amplitude low-frequency oscillations occur for these higher aspect-ratio loops as well as the lower. This typically occurs at a lower velocity with oscillations decreasing in amplitude and increasing in frequency as the freestream velocity is increased. As the velocity is increased, additional energy is imparted to the loop from the freestream flow, and although the oscillations are generally reduced in amplitude and increased in frequency, there remain bursts of large-amplitude oscillations. This increase in "violence" of oscillations is observed at low aspect ratios as well.

At the highest area and aspect ratio the slender teardrop shape begins to occur over the full velocity range. As in the cases of the smaller area loops, the teardrop shape is at its fullest at lower velocities, Fig. 6. For the two areas $A = 0.050$ and 0.075 m^2 at

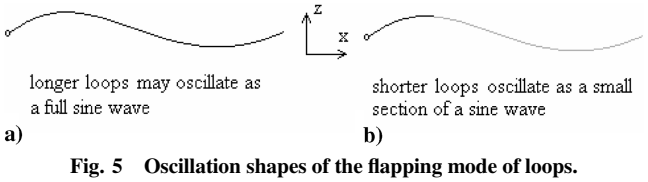

Fig. 5 Oscillation shapes of the flapping mode of loops.

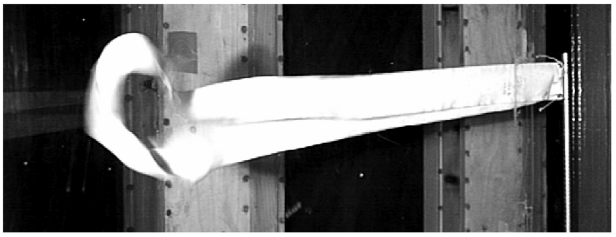

Fig. 6 Loop of $A = 0.075$ m^2 with $AR = 30$ at $U = 6.6$ m/s, $Re = 6.7 \times 10^5$, showing a teardrop shape.

$AR = 30$, twisting of the canopy occurs only at a low velocity. By "twisting" what is meant is canopy inversion. The twisting is not extreme, and at most, one full rotation of the canopy will occur. The problem with this is that once twisted, the canopy will remain deformed. This causes changes in the flutter patterns and the reduction of drag. The teardrop shape is caused by a similar mechanism to that observed in streamers [5,8] and parafoils [8,9]. From these studies it has been observed that at lower Reynolds numbers a streamer will oscillate with increased amplitude and decreased frequency. The shape of this oscillation depends on the length of the streamer, a longer streamer adopting a more sinusoidal-like shape in its flapping mode shape, Fig. 5a. Shorter lengths acquire a straighter canopy orientation, Fig. 5b. The teardrop shape observed in the case of the loops has occurred because each side of the loop behaves like a streamer in its own right. The trailing edges are attached to each other in this case, and this causes the formation of the teardrop shape when the respective trailing edges are moving in opposition to each other.

With an increase in velocity, the teardrop shape becomes thinner and the two sides of the loop only periodically separate, i.e., the loops do not form a permanent teardrop shape. When taking drag measurements it was necessary to test from the higher velocity range to the lower, because in this way the effect of twisting and inversion of the canopy was limited. Twisting could sometimes be overcome by a step increase in velocity, which has the effect of unravelling the loop. However, this did not always solve the problem, and consequently drag measurements at a low velocity tend to show higher degrees of error than those at a higher velocity.

There are, therefore, three distinct canopy orientations that may occur in this low-speed regime: 1) flapping oscillations with damped rotation of the canopy, 2) flapping oscillations with dominant rotation of the canopy, and 3) twisting of the canopy. Within each of these types of oscillation is a velocity and geometry dependant shape of the separation between the loop sides, as outlined in Fig. 4. The combinations of these fluttering properties have direct effect on the drag characteristics of the loops. The formation of a teardrop shape of

a particular streamer at low velocities would cause a larger wake and therefore an increase in the drag coefficient. The higher amplitude oscillations observed at lower velocities will tend to trace out a larger wake and thus should also tend to increase the drag coefficient.

Drag Characteristics

Variation of the Drag Coefficient with Reynolds Number

The effects of the Reynolds number on the drag coefficient are shown in Figs. 7–10. These are grouped into loops with the same aspect ratio. As the Reynolds number decreases, for a given area and aspect ratio there is a general increase in the drag coefficient. At the lowest aspect ratio, AR = 3.3, the data shows a certain sensitivity to the planform area that is not observed at higher aspect ratios. At higher aspect ratios the data from the loops with different areas all collapse onto a single curve approximation, Fig. 11. This clustering was not observed to the same extent for the streamers [5]. In each case, for the same planform geometry, the loop produces a higher drag coefficient than the corresponding streamer. The exception to this rule is the case of AR = 3.3 with $A = 0.025$ m^2, and this case shall be examined later.

For loops, the lower aspect-ratio decelerators behave like streamers, because the loop folds in half to produce a low-aspect-ratio flag. The consequent increased thickness and lower effective aspect ratio (EAR) combine to cause the increase in the drag coefficient. (Note that the effective aspect ratio is found by calculating the aspect ratio of a streamer with half its length, i.e., for loops that fold "perfectly" in half, EAR = AR/2.) At higher aspect ratios the loop sides separate, forming a teardrop shape, causing an

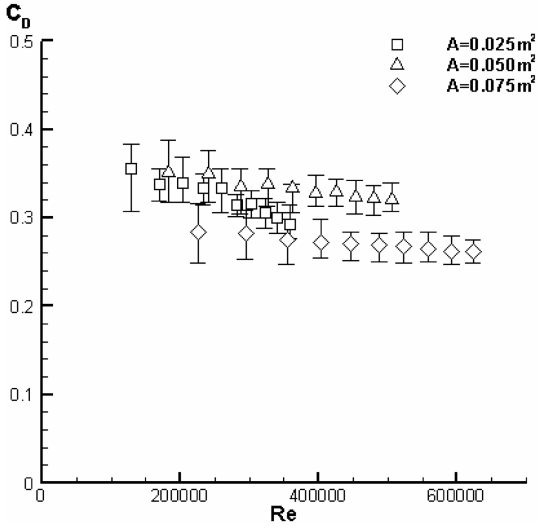

Fig. 7 Drag coefficient versus Reynolds number for loops with AR = 3.3.

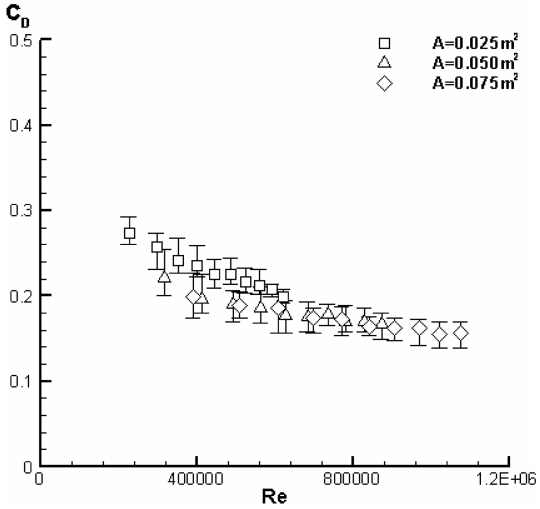

Fig. 8 Drag coefficient versus Reynolds number for loops with AR = 10.

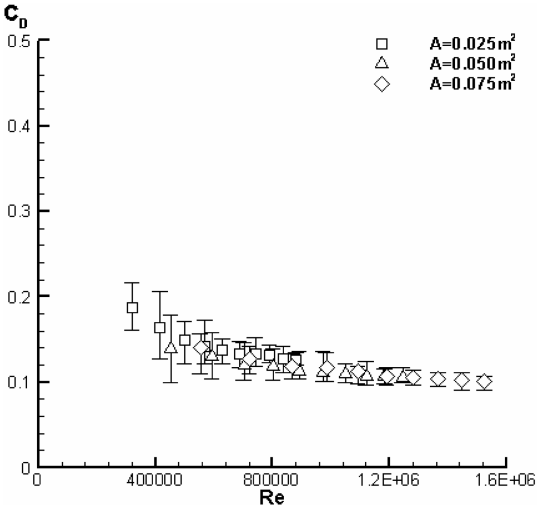

Fig. 9 Drag coefficient versus Reynolds number for loops with AR = 20.

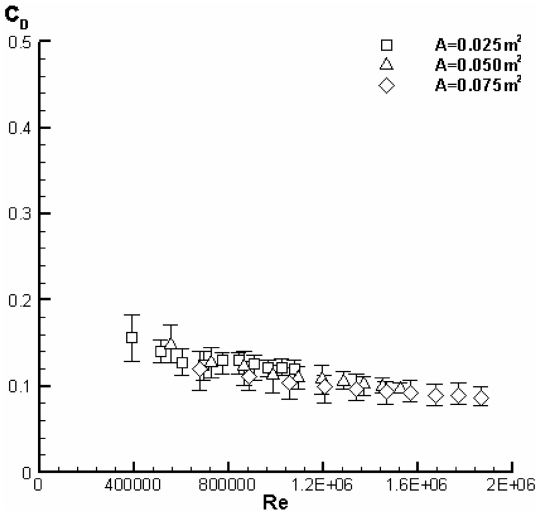

Fig. 10 Drag coefficient versus Reynolds number for loops with AR = 30.

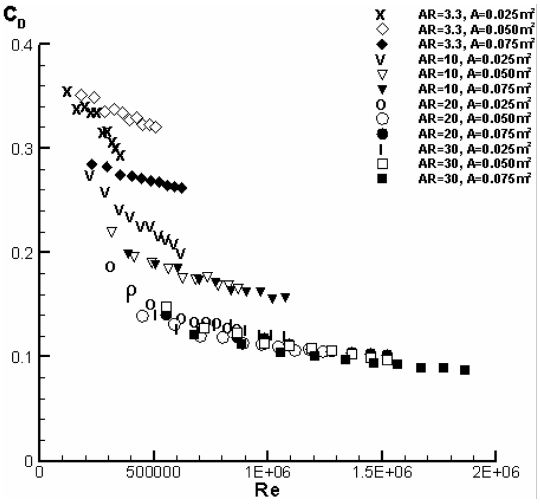

Fig. 11 Drag coefficient versus Reynolds number for all cotton loops.

increase in the loop projected area. At these higher aspect ratios and areas, the flutter characteristics become increasingly sinusoidal. These characteristics cause a larger wake to form and result in increased drag coefficients. At low velocities the teardrop shape becomes particularly exaggerated, and the increase in the drag coefficient becomes sharper than that observed for the streamers. At low aspect ratios and areas, the ratio of amplitude of the oscillation of the loop free edge to the length of the loop, combined with the increased width at the low aspect ratio, served to increase the wake and therefore drag coefficient. This combined effect has a greater influence over the drag coefficient, as the aspect ratio and area are decreased, than does the increased amplitude of oscillation of a similar aspect ratio with a reduction in the Reynolds number.

Variation of the Drag Coefficient with Aspect Ratio

The aspect ratio has a very strong influence over the drag coefficient, Figs. 12–14. At low values, as the aspect ratio increases, there is a sharp drop in the drag coefficient. At higher aspect ratios the drag coefficient levels off. If the aspect ratio was increased further, a minimum drag coefficient of approximately $C_D \approx 0.1$ would be reached. The above general trends would not, however, continue if the aspect ratio was decreased below AR = 3.3. There would instead be a sharp decrease in the drag coefficient [10].

Power series trend lines of the form

$$C_D = c_1 \mathrm{AR}^{c_2} \tag{1}$$

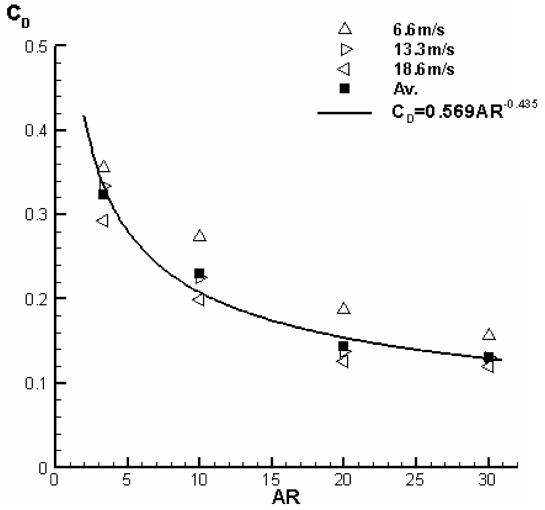

Fig. 12 Drag coefficient versus aspect ratio for loops with $A = 0.025$ m^2.

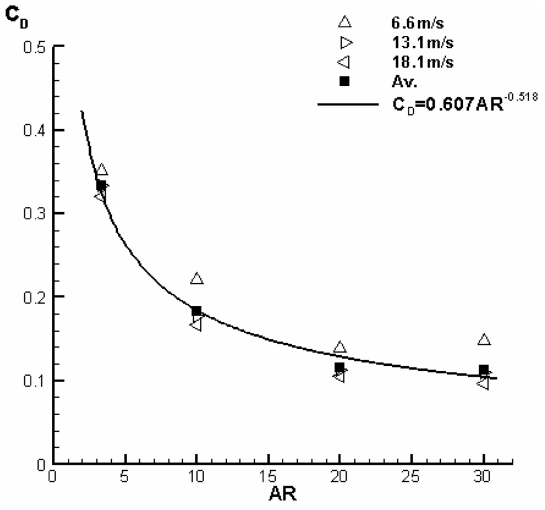

Fig. 13 Drag coefficient versus aspect ratio for loops with $A = 0.050$ m^2.

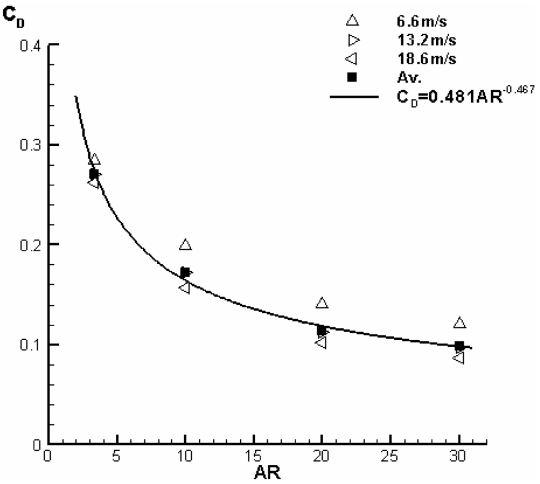

Fig. 14 Drag coefficient versus aspect ratio for loops with $A = 0.075$ m^2.

have been used to approximate the variation of the drag coefficient with aspect ratio. The trend lines become a better fit to the average drag coefficients as the area of the loop is increased. At $A = 0.025$ m^2, the trend line matches less well than in other cases but remains within the range of measured data for each aspect ratio. The loops with the two higher areas produce a large increase in the drag coefficient as the aspect ratio is decreased from AR = 10 to 3.3. This jump is not observed as distinctively for $A = 0.025$ m^2, which shows drag coefficients slightly lower than might be expected, AR = 3.3.

The values c_1 and c_2 do not monotonically increase or decrease with the planform area. Instead a peak is observed in them at $A = 0.050$ m^2, Table 1. The unexpected drop in the drag coefficient for aspect ratio AR = 3.3 and area $A = 0.025$ m^2 is the cause. One might expect the drag coefficients to continue increasing as the area decreases, but as can be seen from Fig. 7, the lowest aspect-ratio data do exhibit different properties.

The effects of the aspect ratio may be examined with respect to other known data [1,3,4], Fig. 15. In this case the definition of the drag coefficient for the streamers and loops has been altered to fit the known data, using a total wetted reference area for calculation of the drag coefficient. (Note that the streamers are defined as rectangular models fixed by a single edge whereas loops have two opposite edges fixed at the same point.) The data obtained in this study show very good agreement with these other data for the streamers, whereas the loop data lies in the mid to upper range. The agreement between the data collected here and the other data taken from studies conducted at much higher velocities is surprising given the notable change in the canopy particularly at low speeds, i.e., the teardrop shape. This canopy shape and changes in the flutter characteristics could account for these results lying in the higher drag coefficient range when placed amongst this other data using nylon. It is also important to note, however, that the nylon fabric used in these other studies, while having similar thickness, may have very different bending rigidity and fabric weight. A lower bending rigidity, by definition, indicates a fabric that is increasingly susceptible to deformations, which would allow increased curvature of the canopy about the x axis and along the loop length. Levin et al [6] have indicated that the material weight is an important factor in determining the drag coefficient of streamers; this would make it an important parameter for loops as well. Additional factors that have not yet been published as affecting the drag coefficient would also need to be taken into account before

Table 1 Variation of the drag coefficient with the aspect ratio for loops described by Eq. (1), coefficients c_1 and c_2

Planform area, m^2	c_1	c_2
0.025	0.569	0.435
0.050	0.607	0.518
0.075	0.481	0.467

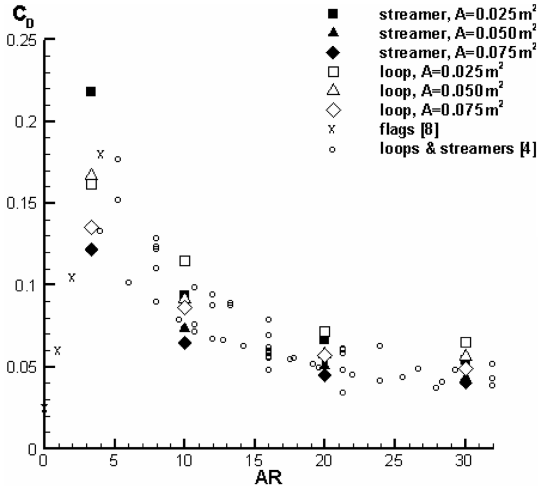

Fig. 15 Drag coefficient based on total wetted area compared with reference data [4,8].

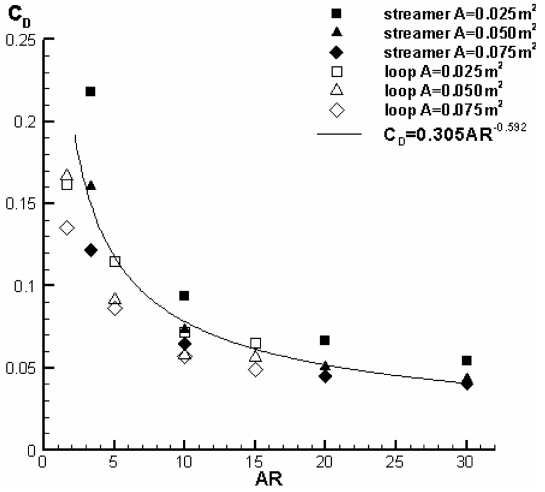

Fig. 16 Drag coefficient versus aspect ratio (streamers) and effective aspect ratio (loops).

isolating material weight and would include the surface of the fabric (surface roughness and weave) and bending hysteresis (recovery of the fabric following deformation). It is certainly true, however, that a lighter material would "catch" in the flow more easily than a heavier material in cases such as those considered here where we have a flexible cantilever, i.e., canopy orientation is horizontal rather than vertical.

The data for the loops and streamers may be replotted as drag coefficient versus aspect ratio, but using the effective aspect ratio for the case of the loops, Fig. 16. By doing this, the single data point that has remained at odds with the rest of the data, $A = 0.025$ m^2 with AR $= 3.3$, suddenly fits very well into the linear trend [10] for flags of AR < 3. The streamers have a sharp rise to a peak in the drag coefficient between AR $= 10$ to 3.3. This peak is also observed for the loop data, as the aspect ratio is decreased. By using an effective area to define the drag coefficient, the loop data fits very well to the linear and subsequent power-law decay. The power law of

$$C_D = 0.305\mathrm{AR}^{-0.592}$$

provides a reasonable fit to the data. It must be remembered, however, that not all loops adopt the streamerlike flutter characteristics. At the highest aspect ratio and highest two areas, the thicker and wider teardrop shapes are formed. However, despite this, the data at the highest aspect ratios and areas actually has closer agreement to the power-law approximation. It must also be pointed out that the data gathered by Auman et al. [1,3,4] used loops and streamers that are significantly longer than those considered here. These other loops exhibited streamerlike characteristics because testing was conducted at the higher velocity range of 27 m/s $< U <$ 46 m/s. The loops investigated here are, therefore, unique in adopting the teardrop shape. This shape is the major cause of the increased drag coefficients compared with those from conventional streamers.

Conclusions

The two mounting rods used during testing of the four types of decelerator have been compared using loops as a test case. The results show reasonable correlation between rods at low aspect ratios and good correlation at medium to high aspect ratios.

At low aspect ratios the loops fold to approximate a flag and their flutter behavior is that of a flag with twice the thickness. The flutter mode is a linear shape or one with very little curvature.

At high aspect ratios the sides of the loops separate, particularly at a low velocity, forming a teardrop shape. The flutter mode is a sinusoidal oscillation.

The drag characteristics mimic those of streamers, with lower Reynolds numbers, aspect ratios, and areas generally producing higher drag coefficients.

The power series trend lines of the form $C_D = c_1(\mathrm{AR})^{-c_2}$ may be used to approximate the variation of the drag coefficient with the aspect ratio, over the range tested.

The drag coefficient has a nonlinear dependency on the planform area. However, as the aspect ratio is increased, the variation becomes closer to a linear function.

When all of the cotton loops and streamers data are plotted as drag coefficient versus Reynolds number, the power series approximation can be clearly seen. When all of the data is plotted as drag coefficient versus aspect ratio, very good agreement with previous data is seen.

Previous loop data has been collected under high velocity conditions, in regimes where loops behave like streamers. The different flutter characteristics observed at lower velocities causes an increase in the drag coefficient. If the current data is replotted using the effective aspect ratio to define the drag coefficient, the linear and power-law decay approximations that have been previously found are observed. A drag coefficient to aspect ratio relationship of $C_D = 0.305\mathrm{AR}^{-0.6}$ has been determined for these low-velocity regimes, for aspect ratios $3 <$ AR < 30.

References

[1] Auman, L. M., Dahlke, C. W., and Purinton, D. C., "Aerodynamic Characteristics of Ribbon Stabilised Grenades," *38th AIAA Aerospace Sciences Meeting and Exhibit*, AIAA Paper 2000-0270, Jan. 2000.

[2] Smith, R., and Shyy, W., "Computation of Aerodynamic Coefficients for a Flexible Membrane Airfoil in Turbulent Flow: A Comparison with Classical Theory," *Physics of Fluids*, Vol. 8, No. 12, 1996, pp. 3346–3353.

[3] Auman, L. M., and Dahlke, C. W., "Drag Characteristics of Ribbons," *16th AIAA Aerodynamic Decelerator Systems Technology Conference and Seminar*, AIAA Paper 2001-2011, May 2001.

[4] Auman, L. M., and Wilks, B. L., "Application of Fabric Ribbons for Drag and Stabilisation," *18th AIAA Aerodynamic Decelerator Systems Technology Conference and Seminar*, AIAA Paper 2005-1618, May 2005.

[5] Carruthers, A. C., and Filippone, A., "Aerodynamic Drag of Streamers and Flags," *Journal of Aircraft*, Vol. 42, No. 4, 2005, pp. 976–982.

[6] Levin, D., Daser, G., and Shpund, Z., "On the Aerodynamic Drag of Ribbons," *14th AIAA Aerodynamic Decelerator Systems Technology Conference*, AIAA Paper 97-1525, June 1997.

[7] Fairthorne, R. A., "Drag of Flags," Aeronautical Research Committee, Rept. and Memorandum 1345, May 1930.

[8] Carruthers, A. C., and Filippone, A., "Aerodynamic Drag of Streamers, Parafoils and Loops," *43rd AIAA Aerospace Sciences Meeting and Exhibit*, AIAA Paper 2005-856, Jan. 2005.

[9] Carruthers, A. C., and Filippone, A., "Aerodynamic Drag of Parafoils," *Journal of Aircraft*, Vol. 42, No. 4, 2005, pp. 1081–1083.

[10] Hoerner, S. F., "Fluid-Dynamic Drag: Practical Information on Aerodynamic Drag and Hydrodynamic Resistance," published by the author, New Jersey, 1958.